Pakistan Veterinary Journal

ISSN: 0253-8318 (PRINT), 2074-7764 (ONLINE)
DOI: 10.29261/pakvetj/2026.249

RESEARCH ARTICLE

DSPE, a Homogeneous Polysaccharide Purified from Durian Shell, Ameliorates Ulcerative Colitis by Restoring Intestinal Epithelial Barrier Function Via the ALG10/AhR/CYP1A1 Signaling Pathways

Xiaotian Xu[1#], Leyi Cui[1#], Xingshu Wei[1#], Mengmeng Yang[1], Renhui Wu[1], Simin Zhang[1], Ying Zhang[2], Mohammed Al-Rasheed[4], Essam H. Ibrahim[5,6], Shiqi Dong[3*] and Yuhui Wang[1*]

[1]School of Pharmacy, Guilin Medical University, Guilin 541199, China; [2]College of Veterinary Medicine, China Agricultural University, Beijing 100193, China; [3]College of Animal Science and Technology, Tarim University, Aral 843300, China; [4]Department of Clinical Sciences, College of Veterinary Medicine, King Faisal University, Al-Ahsa, P.O. Box 400, 31982, Saudi Arabia; [5]Biology Department, Faculty of Science, King Khalid University, P.O. Box 9004, Abha 61413, Saudi Arabia; [6]Blood Products Quality Control and Research Department, National Organization for Research and Control of Biologicals, Cairo, Egypt
[#]These authors contributed equally to this work and are considered as co-first authors
*Corresponding author: tcvm@taru.edu.cn (SD); wangyuhuitg2017@163.com (YW)

ARTICLE HISTORY (26-1170)

Received: September 26, 2026
Revised: October 22, 2026
Accepted: October 28, 2026
Published online: October 30, 2026

Key words:
ALG10/AhR/CYP1A1
Signaling pathway
Durian shell polysaccharide
Ulcerative colitis

ABSTRACT

Ulcerative colitis (UC) is a chronic idiopathic inflammatory bowel disease with complex etiology involving multiple pathological processes including inflammation and oxidative stress. Traditional Chinese medicine polysaccharides show promising prospects in alleviating UC-associated intestinal inflammation but are mostly derived from high-value economic crops or medicinal plants at high cost and their high molecular weights and poor solubility cause low bioavailability, limiting their development and application. Therefore, identifying inexpensive alternative polysaccharide sources with low molecular weight and good water solubility is key to overcoming these bottlenecks. Durian shells, agricultural waste rich in pectic polysaccharides, are widely available at extremely low cost, making them an ideal candidate. Based on this, we isolated and purified durian shell polysaccharide (DSPE), a single component with lower molecular weight and higher water solubility, from durian shells and evaluated its therapeutic potential and mechanism in ameliorating UC using dextran sulfate sodium (DSS)- and lipopolysaccharide (LPS)-induced models. The results showed that 20mg/kg DSPE reduced pro-inflammatory cytokines and oxidative stress, upregulated ZO-1 and Occludin expression, and restored intestinal epithelial barrier function both in vivo and in vitro. Mechanistically, DSPE downregulated ALG10 (asparagine-linked glycosylation 10) while upregulating AhR (aryl hydrocarbon receptor) and CYP1A1 (cytochrome P450 family 1 subfamily A member 1). Administration of an AhR antagonist or ALG10 overexpression aggravated UC symptoms and attenuated the protective effects of DSPE. In summary, these findings indicate that DSPE ameliorates ulcerative colitis by modulating the ALG10/AhR/CYP1A1 signaling pathway to inhibit inflammation and oxidative stress, thereby restoring intestinal epithelial barrier integrity.

To Cite This Article: Xu X, Cui L, Wei X, Yang M, Wu R, Zhang S, Zhang Y, Al-Rasheed M, Ibrahim EH, Dong S and Wang Y, 2026. DSPE, a homogeneous polysaccharide purified from durian shell, ameliorates ulcerative colitis by restoring intestinal epithelial barrier function via the ALG10/AhR/CYP1A1 signaling pathways. Pak Vet J, 46(10): 2336-2351. http://dx.doi.org/10.29261/pakvetj/2026.249

INTRODUCTION

Ulcerative colitis (UC) is a chronic and recurrent gastrointestinal disease occurring in humans and various animal species (Kobayashi *et al*., 2020), characterized by persistent inflammation and ulceration of the colonic mucosa, manifesting as tissue defects or erosions (Li *et al*., 2022; Uwada *et al*., 2023). Current research indicates that the pathogenesis of UC is closely associated with intestinal epithelial cells (IECs) (Xu *et al*., 2022). Under

normal conditions, colonic IECs form an important physical barrier that regulates selective permeability and controls substance transport. They not only allow the smooth passage of water, essential ions, and nutrients to maintain the stability of the internal environment, but also effectively block the invasion of various pathogenic antigens from the intestinal lumen, including endotoxins, viruses, bacteria, and their metabolites, playing a critical role in maintaining intestinal homeostasis and host defense (Schulzke *et al*., 2009). However, during the development of UC, IECs are severely damaged by inflammatory mediators and inflammatory cells in the lamina propria, leading to their destruction, followed by the invasion of harmful substances into the intestinal environment and excessive activation of immune responses. This process leads to intestinal barrier leakage, promotes chronic disease progression, and severely impairs the self-repair capacity of IECs, resulting in severe compromise of the transport and defense functions of the intestinal epithelial barrier, while simultaneously aggravating refractory ulcerative lesions (Martini *et al*., 2017; Neurath, 2019; Kobayashi *et al*., 2020). For example, in mice, UC triggers the release of large amounts of pro-inflammatory mediators that directly damage IECs and induce their apoptosis; reactive oxygen species (ROS) activate inflammasomes leading to excessive immune activation; and the downregulation and disorganized distribution of tight junction proteins increase intestinal barrier permeability, thereby aggravating refractory ulcerative lesions (Li *et al*., 2025). Spontaneous UC in cats can trigger immune dysregulation in the duodenal mucosa, driving excessive activation of local immune responses, while aberrant expression in IECs transforms them from barrier cells into immune targets, exacerbating immune-mediated IEC damage (Waly *et al*., 2004).

Studies have found that inflammation and oxidative stress play crucial roles in UC in humans and various animal species. Under normal conditions, the intestinal environment maintains a tightly regulated baseline level of inflammatory response. ROS in intestinal tissues exert bactericidal effects and participate in intestinal defense functions (Aviello *et al*., 2019). However, when UC occurs, inflammatory factors exacerbate the infiltration of neutrophils and macrophages into tissues (Dong *et al*., 2022). As the inflammatory environment intensifies, pro-inflammatory cytokines trigger excessive ROS production that exceeds the body's antioxidant defense capacity. Excessive ROS oxidize polyunsaturated fatty acids, triggering lipid peroxidation, which increases cell membrane permeability, further disrupting the intestinal mucosal barrier and exacerbating the inflammatory response. This creates a vicious cycle of "inflammation–oxidative stress–barrier damage," which impedes IEC repair and aggravates refractory ulcers (Jeon *et al*., 2020; De Angelis *et al*., 2021).

Therefore, excessive inflammation and oxidative stress are key factors causing intestinal epithelial damage in humans and various animal species. Multiple signaling pathways can ameliorate UC by regulating inflammation and oxidative stress. The aryl hydrocarbon receptor (AhR) is a transcription factor widely expressed in immune system cells. Its signal transduction is an important component of immune responses at barrier sites and plays a key role in maintaining intestinal homeostasis (Zhou *et al*., 2024). AhR influences various aspects of intestinal health, including epithelial renewal and barrier integrity (Lamas *et al*., 2016). Furthermore, as a participant in redox balance and a regulator of redox signaling, AhR regulates the expression of antioxidant system genes, thereby participating in cellular antioxidant defense (Grishanova and Perepechaeva, 2022). Quercetin has been reported to activate AhR in mice, thereby reducing intestinal inflammation, modulating oxidative stress, restoring tight junction integrity, repairing intestinal epithelial barrier dysfunction, and ultimately alleviating UC (Wang *et al*., 2024; Wei *et al*., 2025). Baicalein ameliorates UC by activating AhR in mice to maintain tight junctions and repair the intestinal epithelial barrier (Li *et al*., 2022). Gastrodin alleviates colonic inflammation by activating AhR and inhibiting NLRP3 inflammasome activity in mice (Zhang *et al*., 2025). Fructooligosaccharides increase AhR expression in the mouse colon, further promoting the expression of intestinal tight junction proteins, thereby ameliorating UC (Yang *et al*., 2024). These findings indicate that modulating the AhR signaling pathway is an effective strategy for ameliorating intestinal mucosal barrier damage and UC.

Natural polysaccharides, especially soluble polysaccharides, have been demonstrated to effectively alleviate intestinal inflammation symptoms. Multiple studies have found that Bletilla striata polysaccharide protects the intestinal epithelial barrier by inhibiting inflammatory pathways and oxidative stress (Yue *et al*., 2016; Luo *et al*., 2018; Zhang *et al*., 2019). Lycium barbarum polysaccharide has been confirmed to alleviate chronic colitis by modulating inflammatory cytokines and tight junction proteins (Li *et al*., 2023a). *Tremella fuciformis* polysaccharide ameliorates UC by suppressing inflammation and enhancing intestinal epithelial barrier function. Carthamus tinctorius polysaccharide ameliorates acute UC by inhibiting the secretion of colonic inflammatory factors and restoring the colonic mucosal barrier. These findings consistently demonstrate that natural polysaccharides from different sources exert therapeutic effects on UC through various mechanisms. However, despite the great potential of these polysaccharides in treating intestinal inflammation, their high costs, due to their derivation from high-value economic crops or medicinal plants, have limited their industrial development and application. In view of this, we isolated and purified polysaccharide DSPE from durian shells and investigated its role as a key bioactive component in alleviating UC through the downregulation of ALG10 and upregulation of the AhR/CYP1A1 signaling pathway using *in-vivo* and *in-vitro* colitis models.

MATERIALS AND METHODS

Drugs and Reagents: Durian shells (Malaysian Cat Mountain King) were purchased from Guilin, Guangxi. Materials and methods of the extraction, purification, and characterization analyses of DSPE are provided in the Supplementary Materials. DSS (MP Biomedicals), LPS,

mesalazine, and CH223191 (Sigma-Aldrich), FBS (Nanjing Shenghang), TRIzol and Lipofectamine 3000 (Invitrogen), SYBR Green and FastKing RT Mix (Tiangen), ALG10 plasmid (Shanghai Jikai Gene), ELISA kits for TNF-α/IL-6/IL-10/IL-1β (Dakewe), MPO/T-AOC/MDA/CAT/SOD kits (Nanjing Jiancheng), DAO kit (CUSABIO), and D-lactate kit (Shanghai Future Industrial) were obtained from indicated suppliers. Antibodies: ALG10 (Invitrogen), E-cadherin and AhR (Affinity), CYP1A1/ZO-1/N-cadherin/Occludin/Claudin-7 (Proteintech).

Establishment of animal models and drug intervention: This protocol was approved by the Animal Ethics Committee of Guilin Medical University (GLMC202303027). WT C57BL/6J mice (6-8 weeks, Hunan Silek Jingda) and $ALG10^{+/+}$ mice (Jiangsu GemPharmatech) were housed at 20-26°C, 45%-65% humidity, 12 h light/dark cycle, with one-week acclimatization.

Experiment 1: 36 WT mice were randomly divided into 6 groups (n = 6): normal control, DSS model, DSS + DSPE (10, 20, 40mg/kg), and DSS + mesalazine. Experiment 2: another 30 WT mice were divided into 5 groups (n = 6): normal control, DSS model, DSS + DSPE (40mg/kg), DSS + CH223191 (10mg/kg), and DSS + CH223191 (10 mg/kg)+ DSPE (40mg/kg). Experiment 3: 18 WT and 18 $ALG10^{+/+}$ mice were divided into normal control, DSS model, and DSS + DSPE (40mg/kg) groups for each genotype (n = 6). Colitis was induced by 2.5% DSS in drinking water for 7 days, followed by ultrapure water for 3 days; controls received ultrapure water throughout. DSPE or mesalazine was administered daily by oral gavage (0.1mL/10 g, days 1-10), and CH223191 was injected intraperitoneally daily. Body weight, food/water intake, and feces were recorded daily. On day 11, blood was collected; mice were euthanized; and the spleen and colon were excised, weighed, measured, and stored at -80°C.

Disease Activity Index (DAI) assessment and Histological analysis: Colitis severity was scored based on body weight, fecal consistency, and blood in stool (Li *et al*., 2023b). Colon tissues were fixed in 4% paraformaldehyde, paraffin-embedded, sectioned, H&E stained, and examined under a microscope (Olympus BX53, Japan), and pathological damage was scored according to established criteria (Cheng *et al*., 2024).

Analysis of intestinal permeability in the body: Intestinal permeability was assessed by oral gavage of FITC-dextran (0.3mL, 6mg/10g) after 4 h fasting, and serum fluorescence (ex 485/em 535nM) was measured 3h later using a BioTek Synergy HT reader.

Cell culture: Caco-2 cells were cultured in DMEM with 20% FBS and 1% penicillin-streptomycin at 37°C with 5% CO_2. Cells were transfected with AhR siRNA (5′-UCACAAACUAAUUUAAUCCAA-3′, GenePharma) using Lipofectamine 3000. To induce inflammation, cells were treated with LPS (1μg/mL) for 24h.

Detection of Oxidative Stress Markers, DAO, D-lactate and Cytokines: Oxidative stress markers (MPO, T-AOC, SOD, CAT, MDA), serum DAO and D-lactate, and cytokines (TNF-α, IL-6, IL-1β, IL-10) in colon homogenates and cell supernatants were measured using commercial kits.

Real-Time Reverse Transcription–Polymerase Chain Reaction (qRT-PCR): Relative mRNA levels of target genes, normalized to GAPDH, were quantified by qPCR (SYBR Green, Bio-Rad MyiQ2) and calculated by the $2^{-\Delta\Delta Ct}$ method.

Western blot (WB): Total proteins from colon tissues or Caco-2 cells were separated by 10% SDS-PAGE, transferred to NC membranes, blocked, and probed with primary antibodies overnight, followed by ECL detection.

Statistical analysis: Data (mean±SEM, ≥3 experiments) were analyzed using GraphPad Prism 10.0. One-way ANOVA (Tukey's post-hoc) and two-way ANOVA (Bonferroni's correction) were applied ($P<0.05$).

RESULTS

Structural characterisation: Ion-exchange column chromatography analysis indicated that DSP-C was the target active enrichment component (Fig. 1A). This component was further purified by gel filtration chromatography to obtain the purified sample DSPE. Molecular weight determination revealed that DSPE is a polysaccharide fraction with good homogeneity (Fig. 1B). Its number-average molecular weight (Mn) is 6482Da, weight-average molecular weight (Mw) is 8415 Da, median molecular weight is 4620Da and the dispersity index (Đ, Mw/Mn) is 1.82 (Table 1). Monosaccharide composition analysis indicated that DSPE is primarily composed of galacturonic acid (GalA, 68.1%), rhamnose (13.6%) and galactose (11.0%) (Fig. 1C, Table 2). Methylation analysis revealed that the glycosidic linkage profile of DSPE is dominated by 1,4-linked galacturonic acid (1,4-GalpA, 53.8%). Other major linkages include terminal rhamnose (t-Rhap, 5.5%), 1,2-linked rhamnose (1,2-Rhap, 5.9%), 1,2,4-linked rhamnose (1,2,4-Rhap, 5.1%), terminal glucuronic acid (t-GlcpA, 4.5%), terminal galacturonic acid (t-GalpA, 4.3%), and 1,4-linked galactose (1,4-Galp, 9.1%). Minor linkages such as 1,3-GalpA, 1,3,4-GalpA, 1,2,4-GalpA, 1,4,6-GalpA, 1,3-Rhap, and terminal arabinose (t-Araf) were also detected. Detailed information is provided in the supplementary materials (Table 3). The FT-IR spectrum shows that DSPE exhibits characteristic absorption peaks of polysaccharide chemical bonds and functional groups. The absorption peak at $1613cM^{-1}$ is the characteristic peak of the asymmetric stretching vibration of the free carboxyl group (COO^-) in galacturonic acid. The absorption peak at $1740cM^{-1}$ is significantly weaker than the peak at $1613cM^{-1}$, indicating that the degree of methylation of the polysaccharide sample is relatively low (Fig. 1D).

Table 1: Molecular weight results of sample DSPE

RT (min)	Mp (Da)	Mw (Da)	Mn (Da)	Peak area percentage (%)	Mw/Mn
37.486	6482	8415	4620	100	1.82

Table 2: Molar percentage of each component of DSPE

Man	GlcN	Rha	GlcA	GalA	GalN	Glc	Gal	Xyl	Ara	Fuc
1.861	0.601	13.599	3.051	68.100	0.000	0.819	11.038	0.000	0.931	0.000

Table 3: Glycosidic linkage of DSPE

Glycosidic linkage	PMAA	Mw	RT （min）	Relative molar quantity	Relative molar ratio (%)
t-Araf	1,4-di-O-acetyl-2,3,5-tri-O-methyl arabinitol	279	11.732	608.370	0.798
t-Rhap	1,5-di-O-acetyl-6-deoxy-2,3,4-tri-O-methyl rhamnitol	293	12.777	4160.877	5.458
1,2-Rhap	1,2,5-tri-O-acetyl-6-deoxy-3,4-di-O-methyl rhamnitol	321	15.548	4531.021	5.944
1,3-Rhap	1,3,5-tri-O-acetyl-6-deoxy-2,4-di-O-methyl rhamnitol	321	15.948	610.280	0.801
t-GlcpA	1,5-di-O-acetyl-2,3,4,6-tetra-O-methyl glucitol	325	16.812	3440.157	4.513
t-Galp	1,5-di-O-acetyl-2,3,4,6-tetra-O-methyl galactitol	325	17.512	1085.035	1.423
t-GalpA	1,5-di-O-acetyl-2,3,4,6-tetra-O-methyl galactitol	325	17.512	3296.220	4.324
1,2,4-Rhap	1,2,4,5-tetra-O-acetyl-6-deoxy-3-O-methyl rhamnitol	349	18.450	3887.395	5.100
1,4-Galp	1,4,5-tri-O-acetyl-2,3,6-tri-O-methyl galactitol	351	19.933	6951.262	9.119
1,4-GalpA	1,4,5-tri-O-acetyl-2,3,6-tri-O-methyl galactitol	353	19.933	41023.835	53.815
1,3-Galp	1,3,5-tri-O-acetyl-2,4,6-tri-O-methyl galactitol	351	20.377	1627.615	2.135
1,3,4-GalpA	1,3,4,5-tetra-O-acetyl-2,6-di-O-methyl galactitol	381	22.028	2367.606	3.106
1,2,4-GalpA	1,2,4,5-tetra-O-acetyl-3,6-di-O-methyl galactitol	381	22.610	773.852	1.015
1,4,6-GalpA	1,4,5,6-tetra-O-acetyl-2,3-di-O-methyl galactitol	381	23.586	782.200	1.026
1,3,6-Galp	1,3,5,6-tetra-O-acetyl-2,4-di-O-methyl galactitol	379	24.437	1084.876	1.423

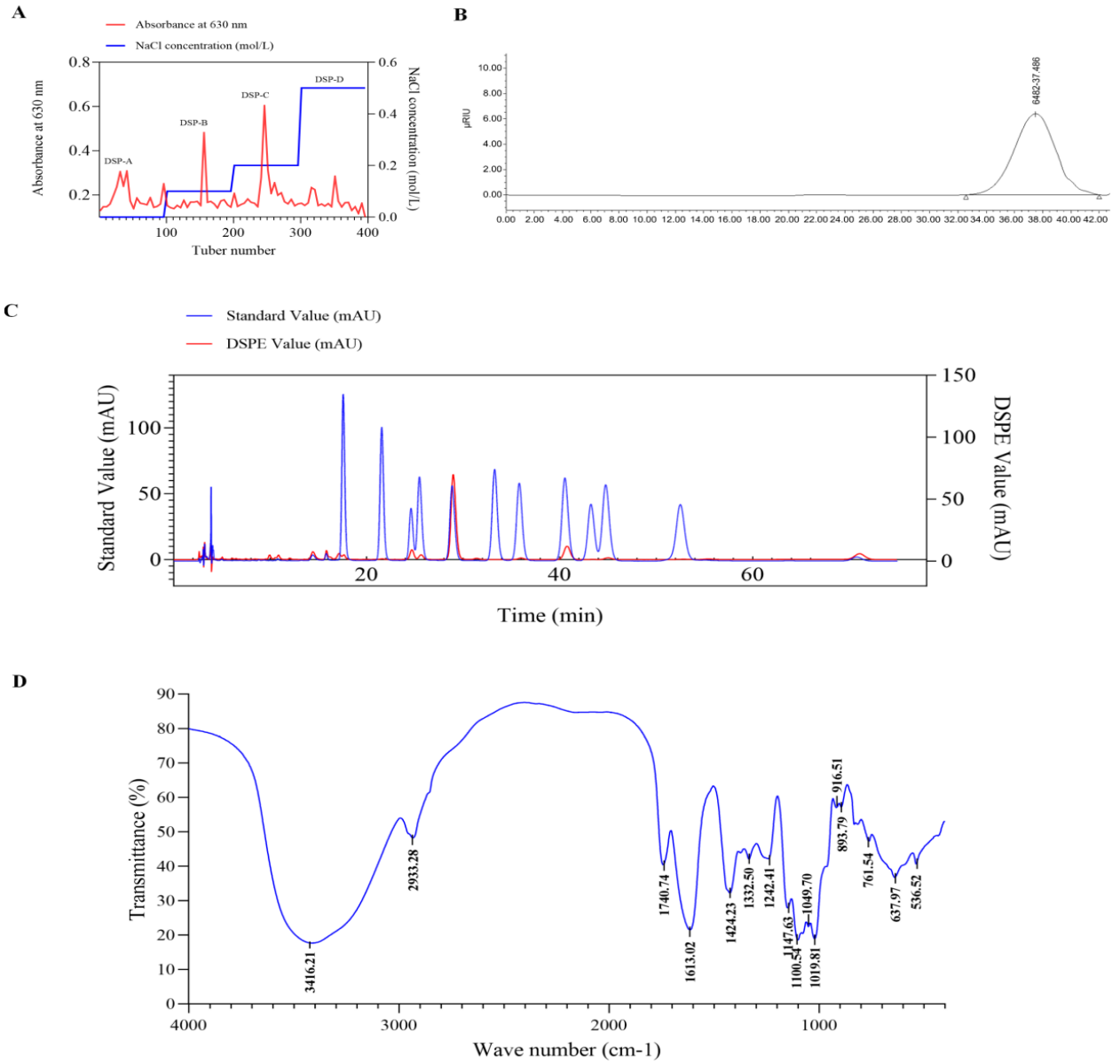


Fig. 1: Isolation, purification process, and basic characterization of DSPE. (A) DSP elution curve. (B) The elution curve of the DSPE sample through gel filtration column chromatography. (C) Monosaccharide composition of DSPE. (D) FT-IR spectra of DSPE.

To further elucidate the structure of DSPE, its glycosidic linkage configurations were analysed by one-dimensional NMR spectroscopy, including ^{1}H-NMR and ^{13}C-NMR and the ^{1}H and ^{13}C chemical shift signals of the major sugar residues were assigned (Fig. 2A-B). The relevant data are provided in the Supplementary Materials (Table 4). The connectivity between individual sugar residues was deduced using two-dimensional NMR spectroscopy, including HSQC, COSY, HSQC-TOCSY, HMBC, and NOESY (Fig. 2C-G). The results showed that DSPE contains a homogalacturonan (HG)-type pectin domain with a chain of →4)-α-D-GalpA-(1→, and O-3 is

connected to an α-D-GalpA-(1→ side chain on the HG-type pectin domain. Additionally, DSPE contains an RG-I type pectin structure. In summary, DSPE is a complex polysaccharide primarily composed of HG and RG-I pectin domains with side chains; a proposed structural unit (Fig. 2H).

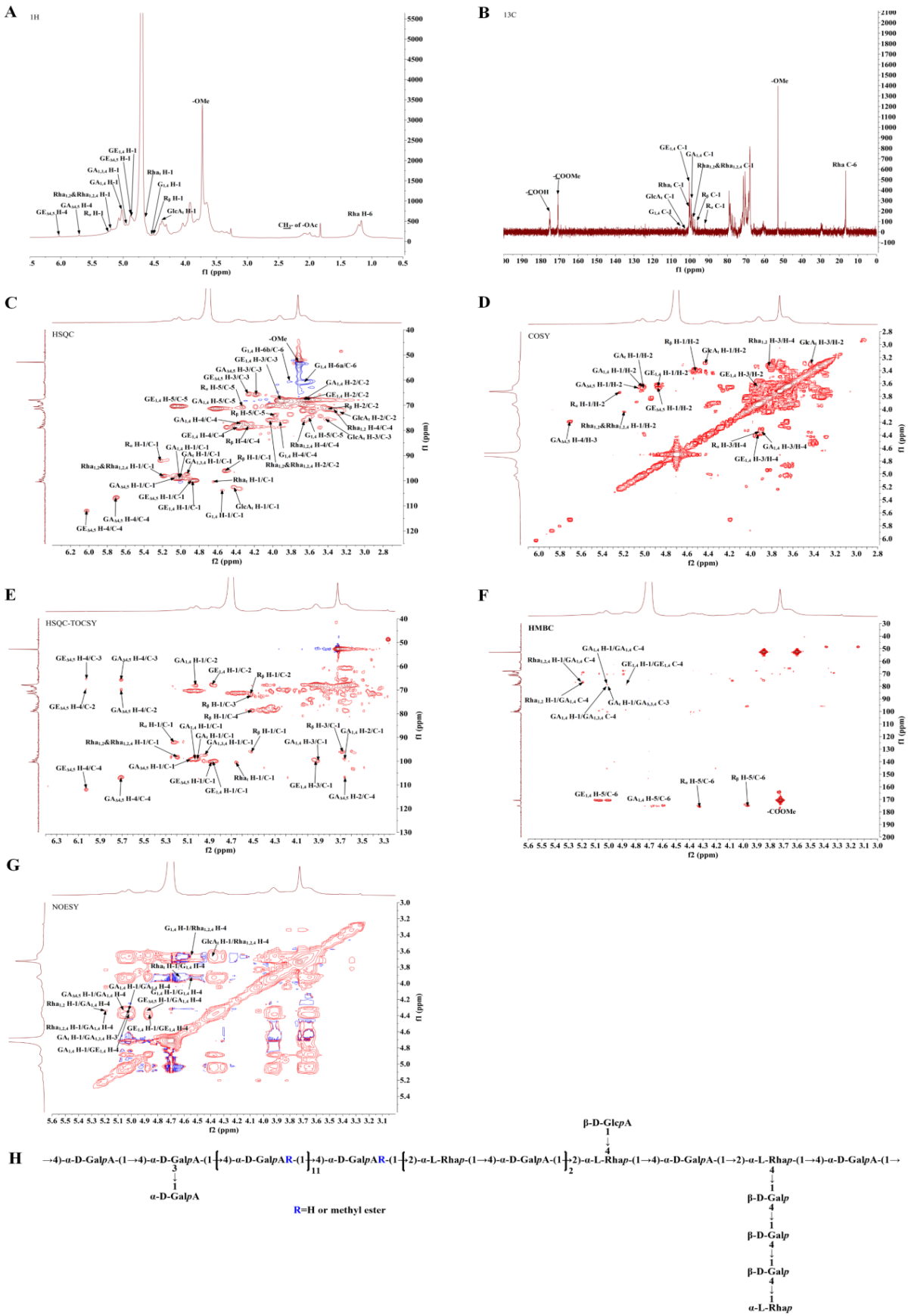


Fig. 2: Structural characterization of DSPE. (A) 1H spectrum of DSPE. (B) 13C spectrum of DSPE. (C) HSQC spectrum of DSPE. (D) COSY spectrum of DSPE. (E) HSQC-TOCSY spectrum of DSPE. (F) HMBC spectrum of DSPE. (G) NOESY spectrum of DSPE. (H) Possible structural units of DSPE.

Table 4: 1H and 13C chemical shift signals of DSPE

Abbreviation	Sugar residue	Chemical shift δ（ppm）						
			1	2	3	4	5	6	-OMe
$GA_{1,4}$	→4)-α-D-Gal*p*A-(1→	H	5.02	3.65	3.90	4.34	4.59/4.63		
		C	99.09	67.88	68.34	77.50	71.17	175.13	
$GA_{1,3,4}$	→3,4)-α-D-Gal*p*A-(1→	H	4.94	3.84	3.98	4.51	4.63		
		C	97.45	67.96	78.94	78.80	71.17	175.13	
GA_t	α-D-Gal*p*A-(1→	H	5.01	3.66	3.81	4.18	4.56		
		C	99.10	67.85	68.53	70.53	71.57	175.28	
$GE_{1,4}$	→4)-α-D-Gal*p*A-6-OMe-(1→	H	4.86	3.64	3.92	4.38	5.00/5.06		3.72
		C	100.39	67.85	68.12	78.68	70.46	170.75	52.84
$GA_{\Delta 4,5}$	α-D-$\Delta^{4,5}$-Gal*p*A-(1→	H	5.05	3.66	4.18	5.70	--	--	
		C	99.30	69.99	65.53	106.84	--	--	
$GE_{\Delta 4,5}$	α-D-$\Delta^{4,5}$-Gal*p*A-6-OMe-(1→	H	4.87	3.68	4.26	6.02	--	--	
		C	100.13	69.52	65.53	112.00	--	--	
R_α	→4)-α-D-Gal*p*A	H	5.22	3.74	3.91	4.34	4.33		
		C	92.05	67.85	68.12	77.55	70.46	175.13	
R_β	→4)-β-D-Gal*p*A	H	4.51	3.41	3.67	4.26	3.97		
		C	96.04	71.40	72.04	78.72	73.98	175.13	
$G_{1,4}$	→4)-β-D-Gal*p*-(1→	H	4.54	3.56	3.67	3.92	3.60	3.65/3.82	
		C	103.79	70.47	72.10	76.38	74.80	60.61	
$Rha_{1,2}$	→2)-α-L-Rha*p*-(1→	H	5.18	4.03	3.83	3.32	3.71	1.16	
		C	98.27	76.04	68.34	71.85	67.85	16.55	
$Rha_{1,2,4}$	→2,4)-α-L-Rha*p*-(1→	H	5.18	4.03	3.98	3.65	3.94	1.21	
		C	98.27	76.04	70.18	76.06	69.57	16.55	
Rha_t	α-L-Rha*p*-(1→	H	4.64	3.83	3.68	3.32	3.93	1.16	
		C	100.27	70.24	69.96	71.85	69.57	16.55	
$GlcA_t$	β-D-Glc*p*A-(1→	H	4.42	3.27	3.43	3.42	3.62		
		C	102.38	72.19	75.70	71.36	76.04	175.29	

The DSPE protective effects on DSS-induced UC mice: To clarify the effective dose of DSPE, we treated model mice with different doses of DSPE (10, 20 and 40mg/kg) (Fig. 3A). As shown in Fig. 3B-H, compared with the model group, the UC symptoms of mice were significantly improved after DSPE treatment, and the therapeutic effect was dose-dependent. The 20 and 40mg/kg dose groups showed the most significant effects. These results indicate that DSPE effectively alleviates UC symptoms in a dose-dependent manner within a certain range.

DSPE inhibits DSS-induced colonic inflammation and oxidative stress, thereby improving intestinal epithelial dysfunction: Inflammation and oxidative stress can lead to DNA damage and abnormal apoptosis in IECs, thereby disrupting the intestinal epithelial barrier. As shown in Fig. 4A-P, DSS treatment significantly increased the protein and mRNA expression levels of pro-inflammatory factors (TNF-α, IL-1β and IL-6), as well as the levels of MDA, MPO, FITC-D, DAO, and D-lactate. In contrast, the protein and mRNA expression levels of the anti-inflammatory factor IL-10 and the levels of T-AOC, SOD and CAT were significantly reduced. Conversely, DSPE treatment significantly decreased the protein and mRNA expression levels of pro-inflammatory factors, reduced the levels of MDA, MPO, FITC-D, DAO and D-lactate, whilst significantly increasing the protein and mRNA expression levels of the anti-inflammatory factor and elevating the levels of T-AOC, SOD, and CAT. These results indicate that DSPE inhibits inflammation and oxidative damage in UC, regulates intestinal permeability, and is closely related to intestinal epithelial barrier function and integrity.

To further confirm whether DSPE alleviates UC by protecting intestinal epithelial function, we established an LPS-induced intestinal epithelial barrier dysfunction model in Caco-2 cells and treated them with different doses of DSPE (2, 4 and 8μg/mL) to evaluate DSPE's anti-inflammatory and antioxidant properties *in-vitro*. As shown in Fig. 5A-L, LPS significantly increased the protein and mRNA expression levels of pro-inflammatory factors and MDA levels in Caco-2 cells, whilst significantly decreasing the protein and mRNA expression levels of anti-inflammatory factors and the levels of T-AOC, SOD, and CAT. Following DSPE treatment, the protein and mRNA expression levels of pro-inflammatory factors were significantly inhibited, MDA levels were significantly reduced and the protein and mRNA expression levels of anti-inflammatory factors and the levels of T-AOC, SOD and CAT were significantly increased. These *in-vitro* results were consistent with the *in-vivo* findings. Notably, the high-dose DSPE group (8μg/mL) showed the most significant reversal of these changes. These results suggest that DSPE inhibits inflammation and oxidative stress and improves intestinal epithelial barrier dysfunction.

DSPE regulates the ALG10/AHR/CYP1A1 signalling pathway: Previous studies have found that ALG10 is significantly upregulated in CRC tissues and is associated with shortened survival periods in CRC patients (Xu *et al*., 2022). Activation of AhR can regulate the expression and distribution of tight junction proteins and improve intestinal epithelial dysfunction. AhR can target CYP450 family 1 enzymes, and AhR activation upregulates CYP1A1 expression. Therefore, we investigated whether DSPE mediates intestinal barrier protection in UC mice through the ALG10/AhR/CYP1A1 signalling pathway. Western blot and quantitative real-time polymerase chain reaction results (Fig. 6A-G) showed that DSS treatment significantly increased ALG10 protein and mRNA expression levels in colon tissues, whilst significantly

decreasing AhR and CYP1A1 protein and mRNA expression levels. In contrast, DSPE treatment significantly decreased ALG10 protein and mRNA expression levels whilst significantly increasing AhR and CYP1A1 protein and mRNA expression levels. Subsequently, we evaluated whether DSPE regulates the ALG10/AhR/CYP1A1 signalling pathway *in-vitro* (Fig. 6H-N). As expected, the *in-vitro* results were consistent with the *in-vivo* findings.

Inhibition of AhR reversed the intestinal protective effect of DSPE: To determine whether DSPE exerts its protective effect on the intestine through AhR, the effect of CH223191 on DSPE's intestinal protective effects was investigated. The results (Fig. 7A-B and 8A-F) demonstrated that DSPE ameliorated UC in mice by attenuating pathological inflammation and crypt damage in colonic tissues, preserving colon length, enhancing T-AOC, and suppressing the expression of inflammatory cytokines; however, these effects were reversed upon administration of CH223191. Compared with the DSPE monotherapy group, the CH223191 and DSPE combination treatment group showed significantly increased histological scores and TNF-α/IL-6 mRNA expression, as well as significantly shortened colon length and decreased T-AOC levels. Additionally, we measured the mRNA and protein expression of ALG10 and CYP1A1 in the mouse colon tissue, as well as the expression of intestinal barrier-related factors (ZO-1, N-cadherin, E-cadherin, Occludin, and Claudin-7) in the presence of CH223191. The results (Fig. 8G-U) showed that compared with the DSPE monotherapy group, the CH223191 and DSPE combination treatment group significantly decreased the mRNA and protein expression levels of CYP1A1, ZO-1, E-cadherin, Occludin, and Claudin-7, whilst significantly increasing N-cadherin mRNA and protein expression levels. However, the CH223191 and DSPE combination treatment did not significantly alter ALG10 mRNA and protein expression levels.

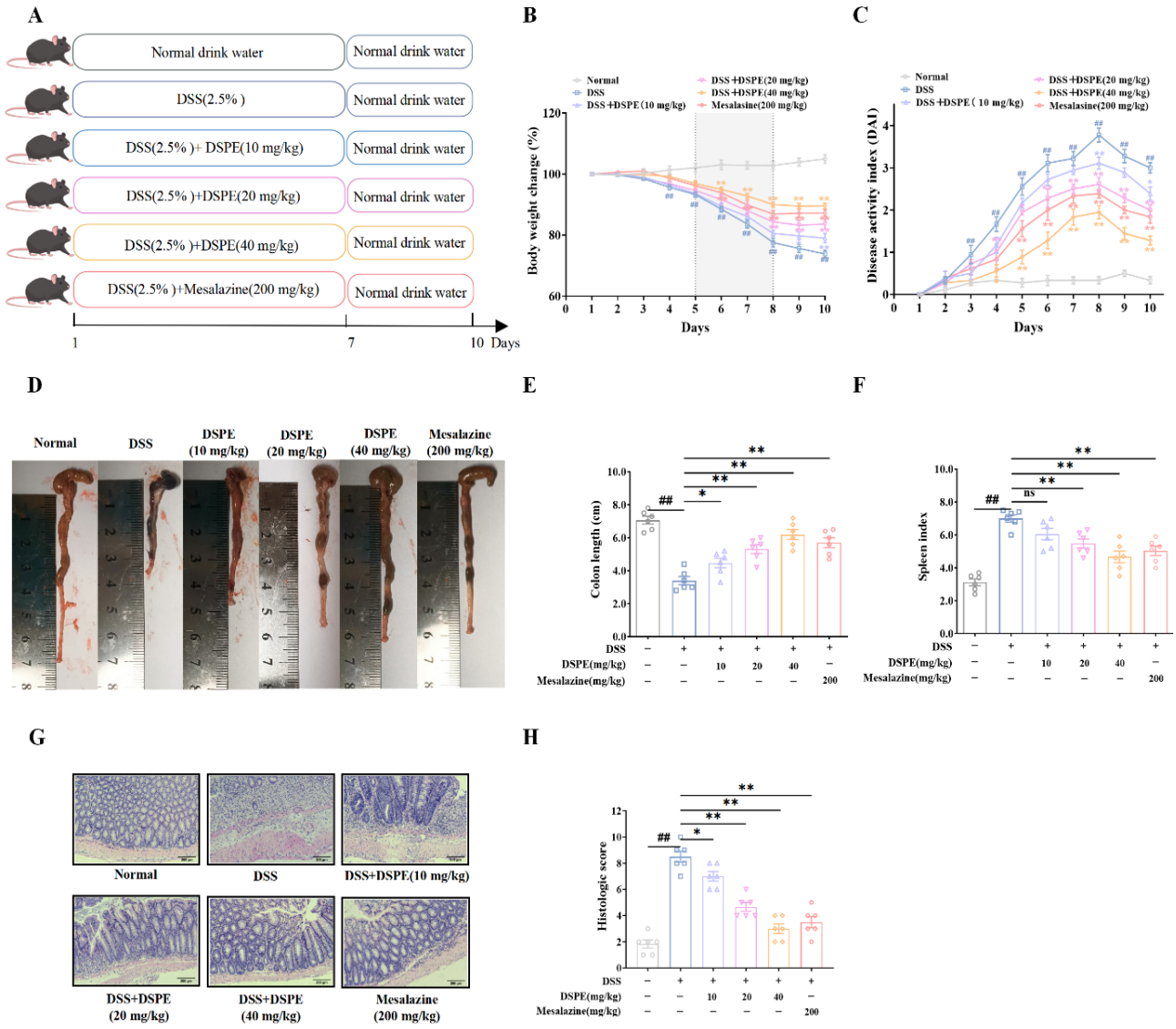


Fig. 3: The effect of different doses of DSPE on the improvement of symptoms of acute colitis in mice caused by DSS. (A) Experimental grouping and flowchart. (B) The percentage change in body weight of mice in each group. (C) DAI score. (D) Representative image of the colon. (E) Colon length. (F) Spleen index. (G) Representative H&E staining of colon tissue images (200×). (H) Histopathological score. Statistical data are presented as mean ± SEM; ##P<0.01 compared with the Normal group; *P<0.05, **P<0.01 compared with DSS group; ns indicates P>0.05.

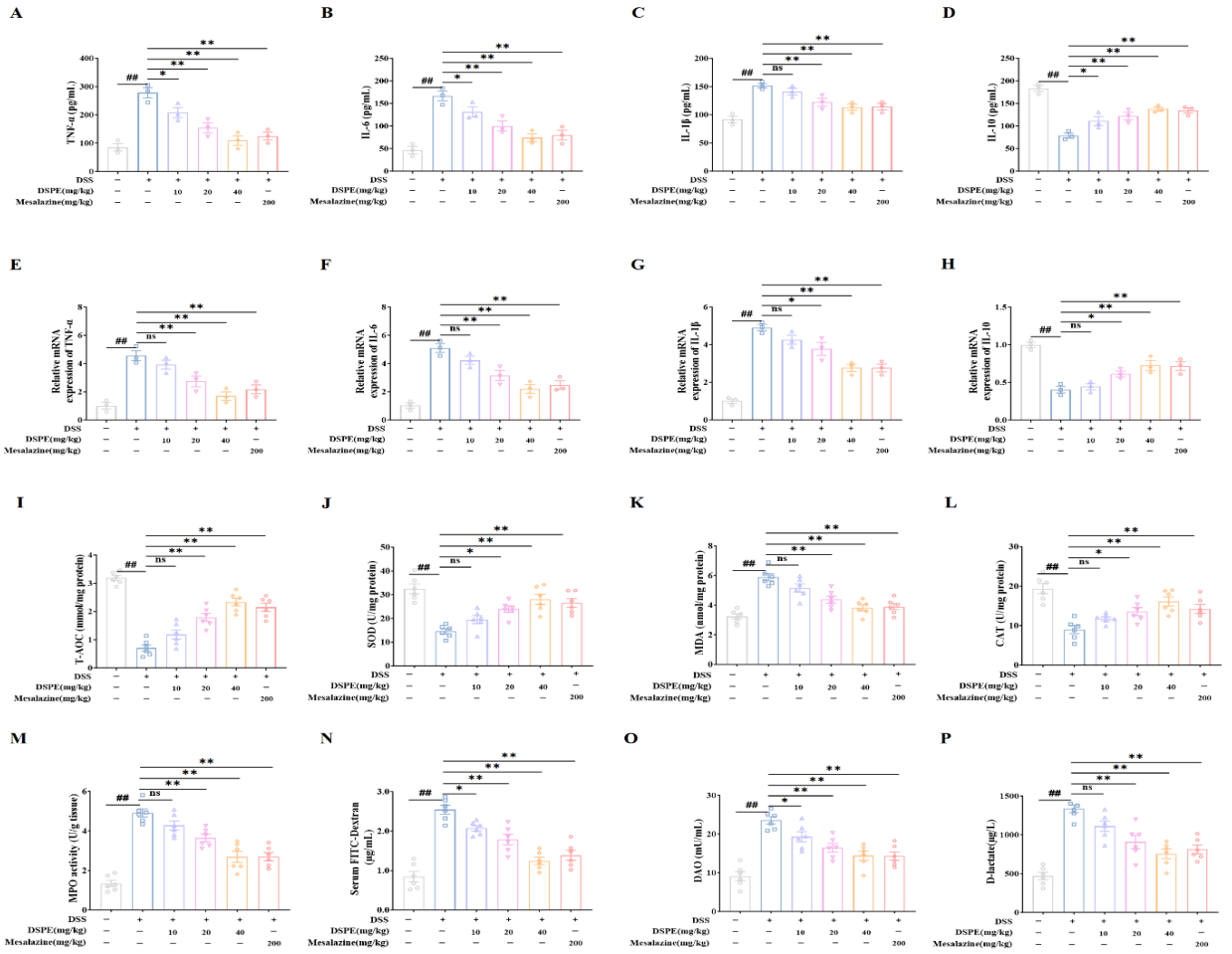


Fig. 4: Impact of DSPE on inflammatory cytokines and oxidative stress biomarkers in DSS-induced colitis mice. (A-D) Expression levels of TNF-α, IL-6, IL-1β, and IL-10 proteins in colon tissue. (E-H) mRNA expression levels of TNF-α, IL-6, IL-1β and IL-10 in colon tissue. (I-M) The levels of T-AOC, SOD, CAT, MDA, and MPO in colon tissues. (N-P) The contents of FITC-D, DAO, and D-lactate in mouse serum. Statistical data are presented as mean ± SEM; ##P<0.01 compared with the Normal group; *P<0.05, **P<0.01 compared with DSS group; ns indicates P>0.05.

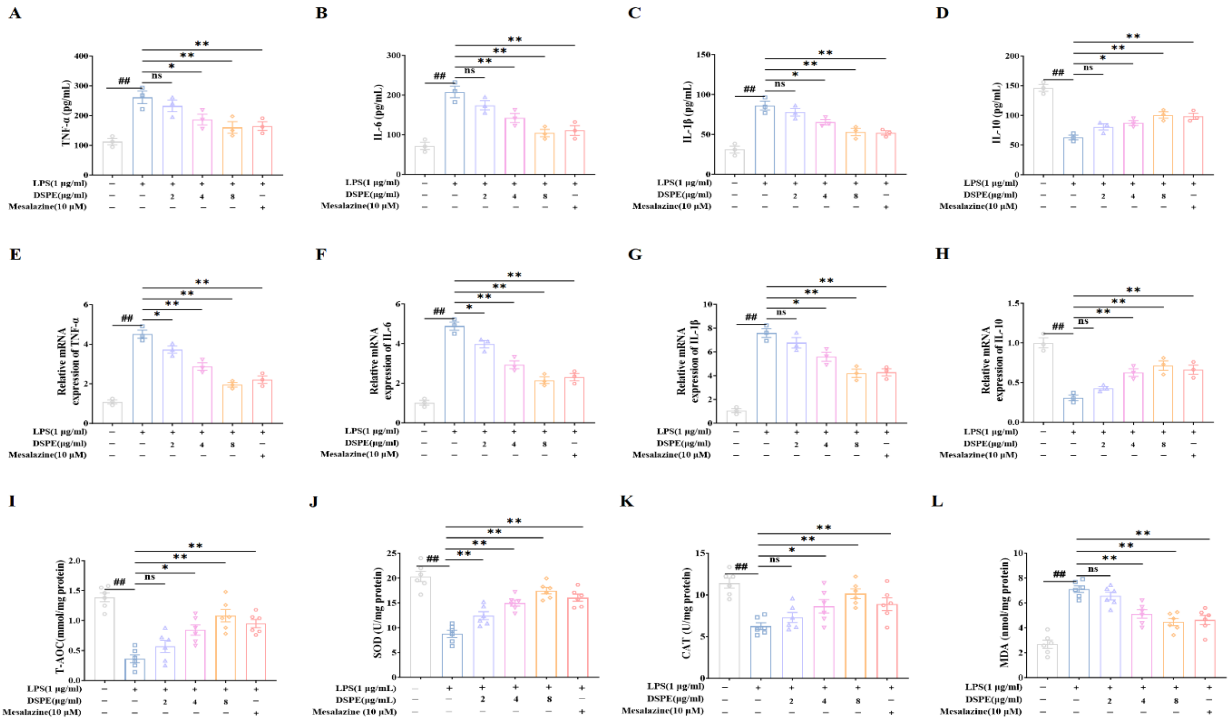


Fig. 5: The *in-vitro* effects of DSPE on oxidative stress markers and inflammatory factors. (A-D) The protein expression levels of TNF-α, IL-6, IL-1β, and IL-10 in Caco-2 cells. (E-H) The mRNA expression levels of TNF-α, IL-6, IL-1β, and IL-10 in Caco-2 cells. (I-L) The levels of T-AOC, SOD, CAT, and MDA in Caco-2 cells. Statistical data are presented as mean ± SEM; ##P<0.01 compared with the Normal group; *P<0.05, **P<0.01 compared with DSS group; ns indicates P>0.05.

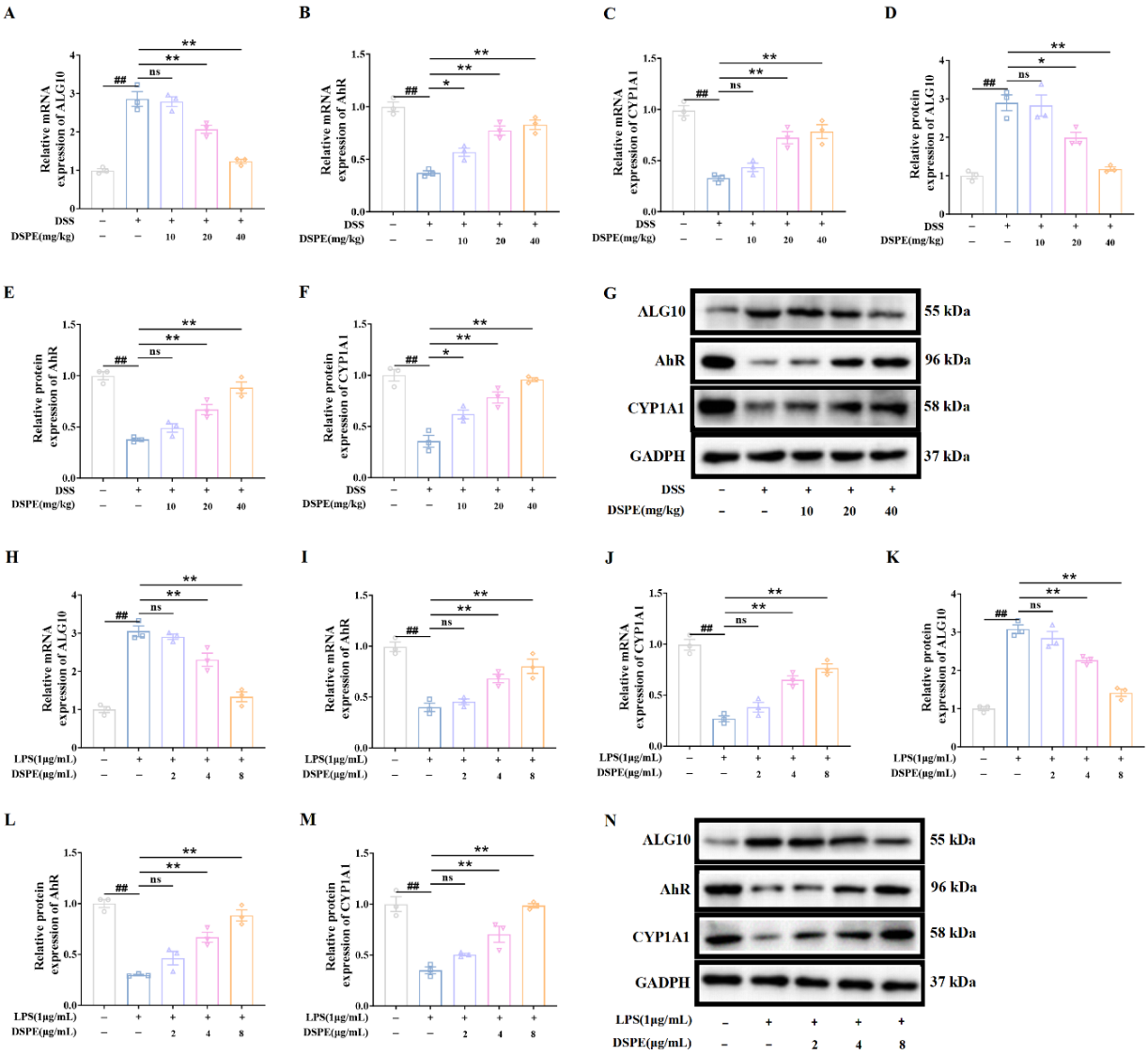


Fig. 6: The influence of DSPE on the expression of factors related to the ALG10/AhR/CYP1A1 signaling pathway in the mouse enteritis model induced by DSS and the injury model of epithelial barrier dysfunction of Caco-2 cells induced by LPS. (A-C) The mRNA expression levels of ALG10, AhR, and CYP1A1 in colon tissues. (D-F) The relative protein expression levels of ALG10, AhR, and CYP1A1 in colon tissues. (G) Representative WB images of ALG10, AhR, and CYP1A1 in colon tissues. (H-J) The mRNA expression levels of AhR and CYP1A1 in Caco-2 cells. (K-M) The relative protein expression levels of ALG10, AhR, and CYP1A1 in Caco-2 cells. (N) Representative WB images of ALG10, AhR, and CYP1A1 in Caco-2 cells. Statistical data are presented as mean ± SEM; $^{\#\#}$P<0.01 compared with the Normal group; *P<0.05, **P<0.01 compared with DSS group; ns indicates P>0.05.

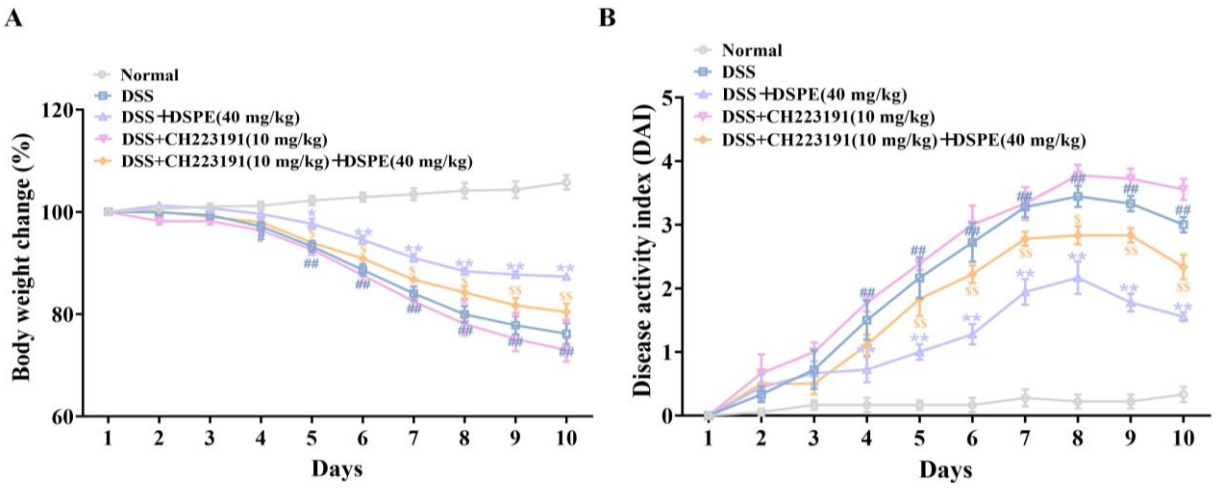


Fig. 7: (A) The percentage change in body weight of mice in each group. (B) DAI score. Statistical data are presented as mean ± SEM; $^{\#\#}$P<0.01 compared with the Normal group; *P<0.05, **P<0.01 compared with the DSS group; $^{\$}$P<0.05, $^{\$\$}$P<0.01 compared with the DSS + DSPE (40mg/kg) group; ns indicates P>0.05.

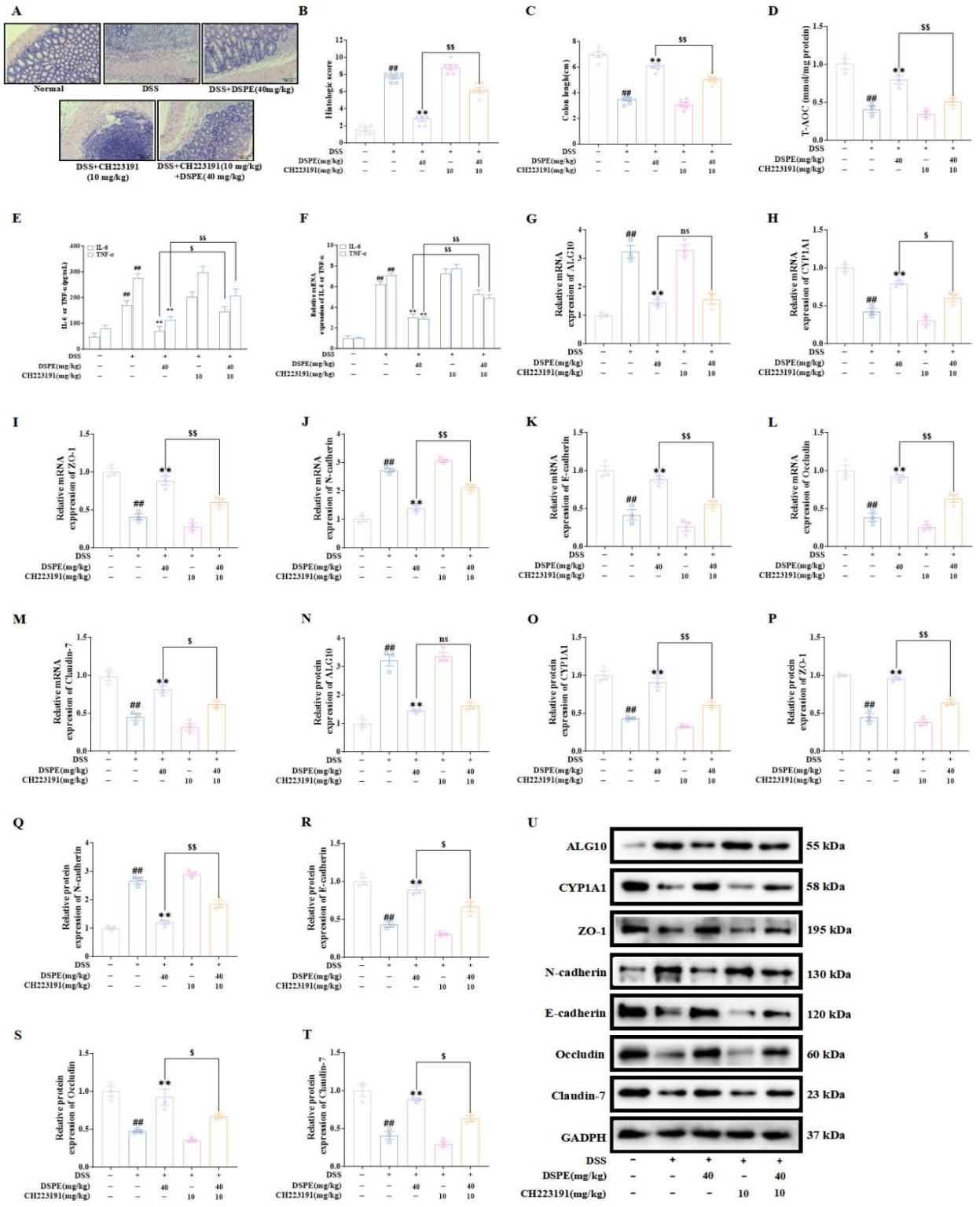


Fig. 8: The effect of AhR on the improvement of UC colonic inflammation, oxidative stress, and intestinal epithelial dysfunction by DSPE. (A) Representative colonic tissue H&E staining images (200×). (B) Histopathological score. (C) Colon length. (D) The level of T-AOC in colon tissue. (E) The protein expression levels of TNF-α and IL-6 in colonic tissues. (F) The mRNA expression levels of TNF-α and IL-6 in colonic tissues. (G-M) The relative mRNA expression levels of ALG10, CYP1A1, ZO-1, N-cadherin, E-cadherin, Occludin, and Claudin-7 in colon tissues. (N-T) Relative protein expression levels of ALG10, CYP1A1, ZO-1, N-cadherin, E-cadherin, Occludin, and Claudin-7 in colon tissues. (U) Representative WB images of ALG10, CYP1A1, ZO-1, N-cadherin, E-cadherin, Occludin, and Claudin-7 in Caco-2 cells. Statistical data are presented as mean ± SEM; $^{\#\#}$P<0.01 compared with the Normal group; *P<0.05, **P<0.01 compared with the DSS group; $^{\$}$P<0.05, $^{\$\$}$P<0.01 compared with the DSS + DSPE (40mg/kg) group; ns indicates P>0.05.

To further investigate the role of AhR in DSPE-mediated maintenance of intestinal epithelial barrier integrity, we induced Caco-2 cells with LPS and simultaneously silenced AhR expression by transfecting siAhR. The results (Fig. 9A-R) showed that compared with the DSPE treatment alone group, AhR silencing significantly increased TNF-α and IL-6 protein expression levels, while significantly decreasing the levels of

CYP1A1, ZO-1, E-cadherin, Occludin, and Claudin-7 and significantly increasing N-cadherin mRNA and protein expression levels. Additionally, AhR silencing did not significantly alter ALG10 mRNA and protein expression levels. These results are consistent with the in vivo findings. AhR antagonist treatment significantly counteracted the beneficial effects of DSPE in DSS-induced UC mice and LPS-induced Caco-2 cells, further demonstrating that DSPE improves intestinal epithelial barrier dysfunction in UC by activating AhR.

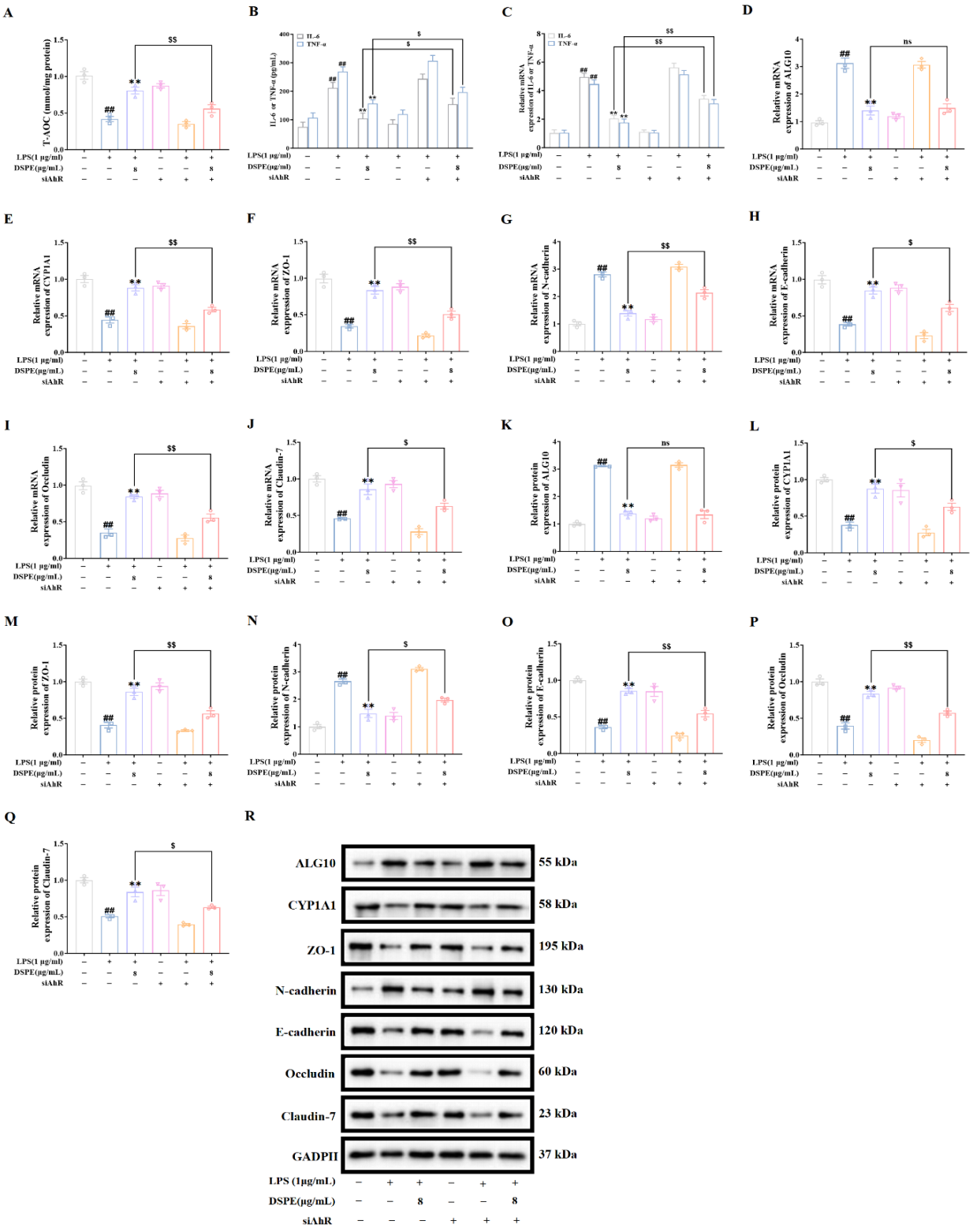


Fig. 9: The effect of AhR on the improvement of inflammation, oxidative stress, and intestinal epithelial dysfunction in Caco-2 cells by DSPE. (A) The T-AOC level of Caco-2 cells. (B) The protein expression levels of TNF-α and IL-6 in Caco-2 cells. (C) The mRNA expression levels of TNF-α and IL-6 in Caco-2 cells. (D-J) The relative protein expression levels of ALG10, CYP1A1, ZO-1, N-cadherin, E-cadherin, Occludin, and Claudin-7 in Caco-2 cells. (K-Q) The relative protein expression levels of ALG10, CYP1A1, ZO-1, N-cadherin, E-cadherin, Occludin, and Claudin-7 in Caco-2 cells. (R) Representative WB images of ALG10, CYP1A1, ZO-1, N-cadherin, E-cadherin, Occludin, and Claudin-7 in Caco-2 cells. Statistical data are presented as mean ± SEM; $^{\#\#}$P<0.01 compared with the Normal group; *P<0.05, **P<0.01 compared with the DSS group; $^{\$}$P<0.05, $^{\$\$}$P<0.01 compared with the LPS + DSPE (8mg/kg) group; ns indicates P>0.05.

The high expression of ALG10 effectively reverses the beneficial effect of DSPE: To assess the crucial role of ALG10 in the DSPE-mediated UC amelioration, both C57BL/6J WT mice and ALG10$^{+/+}$ mice were used. The results (Fig. 10A-B and 11A-C) showed that C57BL/6J WT mice treated with DSPE exhibited significant improvements, including a significant reduction in tissue scores and less pronounced colonic shortening. However, these beneficial effects were attenuated in ALG10$^{+/+}$ mice. Compared with C57BL/6J WT mice treated with DSPE, ALG10$^{+/+}$ mice treated with DSPE showed significantly decreased T-AOC levels (Fig. 11D), while showing significantly increased TNF-α and IL-6 protein and mRNA expression levels (Fig. 11E and F). Additionally, compared with DSPE-treated WT mice, DSPE-treated ALG10$^{+/+}$ mice showed significantly decreased mRNA and protein expression levels of AhR, CYP1A1, ZO-1, E-cadherin, Occludin, and Claudin-7, as well as significantly decreased N-cadherin mRNA and protein expression levels, indicating that ALG10 overexpression reversed these beneficial effects of DSPE. Moreover, we also observed that ALG10 overexpression altered AhR mRNA and protein expression levels, further demonstrating that AhR may be located downstream of ALG10 and upstream of CYP1A1 (Fig. 11G-U).

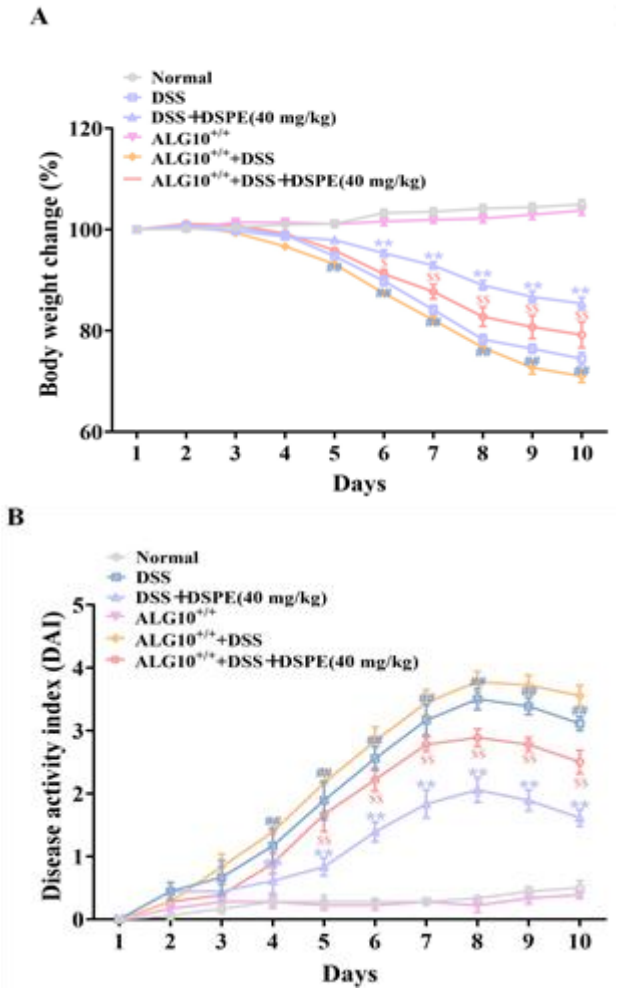


Fig. 10: (A) The percentage change in body weight of mice in each group. (B) DAI score. Statistical data are presented as mean ± SEM; ##P<0.01 compared with the Normal group; *P<0.05, **P<0.01 compared with the DSS group; $P<0.05, $$P<0.01 compared with the DSS + DSPE (40mg/kg) group; ns indicates P>0.05.

To further determine the effect of ALG10 on DSPE-mediated improvement of intestinal epithelial dysfunction, Caco-2 cells were induced with LPS, and ALG10 was overexpressed through transient transfection. As shown in Fig. 12A-R, ALG10 overexpression counteracted DSPE-mediated inhibition of TNF-α and IL-6 at both protein and mRNA levels, and also inhibited the DSPE-induced increase in T-AOC. Moreover, ALG10 overexpression significantly inhibited the DSPE-induced increase in AhR, CYP1A1, ZO-1, E-cadherin, Occludin, and Claudin-7 mRNA and protein expression levels. These results are consistent with the *in-vivo* findings, indicating that ALG10 overexpression effectively reverses DSPE's protective effect on intestinal epithelial dysfunction in UC, suggesting that ALG10 plays an indispensable role in DSPE-mediated UC protection.

DISCUSSION

Although natural polysaccharides possess various biological activities, their relatively high molecular weights and poor solubility lead to low bioavailability, limiting their further development and application (Liu *et al.*, 2025). Studies have found that low-molecular-weight polysaccharides, due to reduced intra- and intermolecular aggregation, expose more active sites and are more easily absorbed by cells, thereby effectively exerting biological activities (Sun *et al*., 2023). For example, Sun *et al*. purified the BBG1 fraction from crude baker's yeast polysaccharides, which showed superior anti-inflammatory activity in mice due to its low molecular weight and high solubility in water (Sun *et al*., 2019). Similarly, Xu *et al*. also confirmed that the low-molecular-weight fraction of Ganoderma lucidum polysaccharide was superior to the original polysaccharide in enhancing antioxidant enzyme activity in mice (Xu *et al*., 2019). Notably, in traditional uses such as soup preparation, only partial water-soluble components can be extracted from durian shells, while the remainder is often discarded. We hypothesized that if a single durian shell polysaccharide DSPE with a smaller molecular weight and higher water solubility could be further isolated and purified from durian shells, its anti-UC efficacy might be significantly enhanced. Based on this hypothesis, our team isolated and purified DSPE, a single polysaccharide with relatively high water solubility, from durian shells. On this basis, the present study further elucidated the mechanism of action of DSPE, providing an important scientific basis for the high-value utilization of durian shell agricultural waste and offering strong support for its development in the field of animal intestinal health.

Dong *et al*. demonstrated that repairing inflammation- and oxidative stress-mediated damage to the intestinal epithelial barrier is a key strategy for treating UC (Dong *et al*., 2024). The mechanism by which modified Gegen Qinlian Decoction treats UC involves inhibiting inflammatory responses, attenuating oxidative stress, and repairing intestinal barrier damage (Wang *et al*., 2023). Huanglian Pingwei San ameliorates UC by reducing inflammation and oxidative stress, and alleviating DSS-induced intestinal barrier damage (Dong *et al*., 2024). Anemoside B4 activates AhR, effectively reducing intestinal oxidative stress and inflammation, enhancing intestinal barrier integrity, and ultimately

ameliorating UC (Wu *et al*., 2025). The present study primarily investigated the mechanism by which DSPE ameliorates intestinal mucosal barrier damage in mice. Our results demonstrated that DSPE significantly downregulated the levels of inflammatory factors (TNF-α and IL-6), while upregulating T-AOC and the expression of intestinal mucosal barrier marker proteins (ZO-1, E-cadherin, Occludin, Claudin-7). These results strongly suggest that the molecular mechanism by which DSPE ameliorates UC involves suppressing inflammatory responses and oxidative stress while repairing colonic mucosal damage.

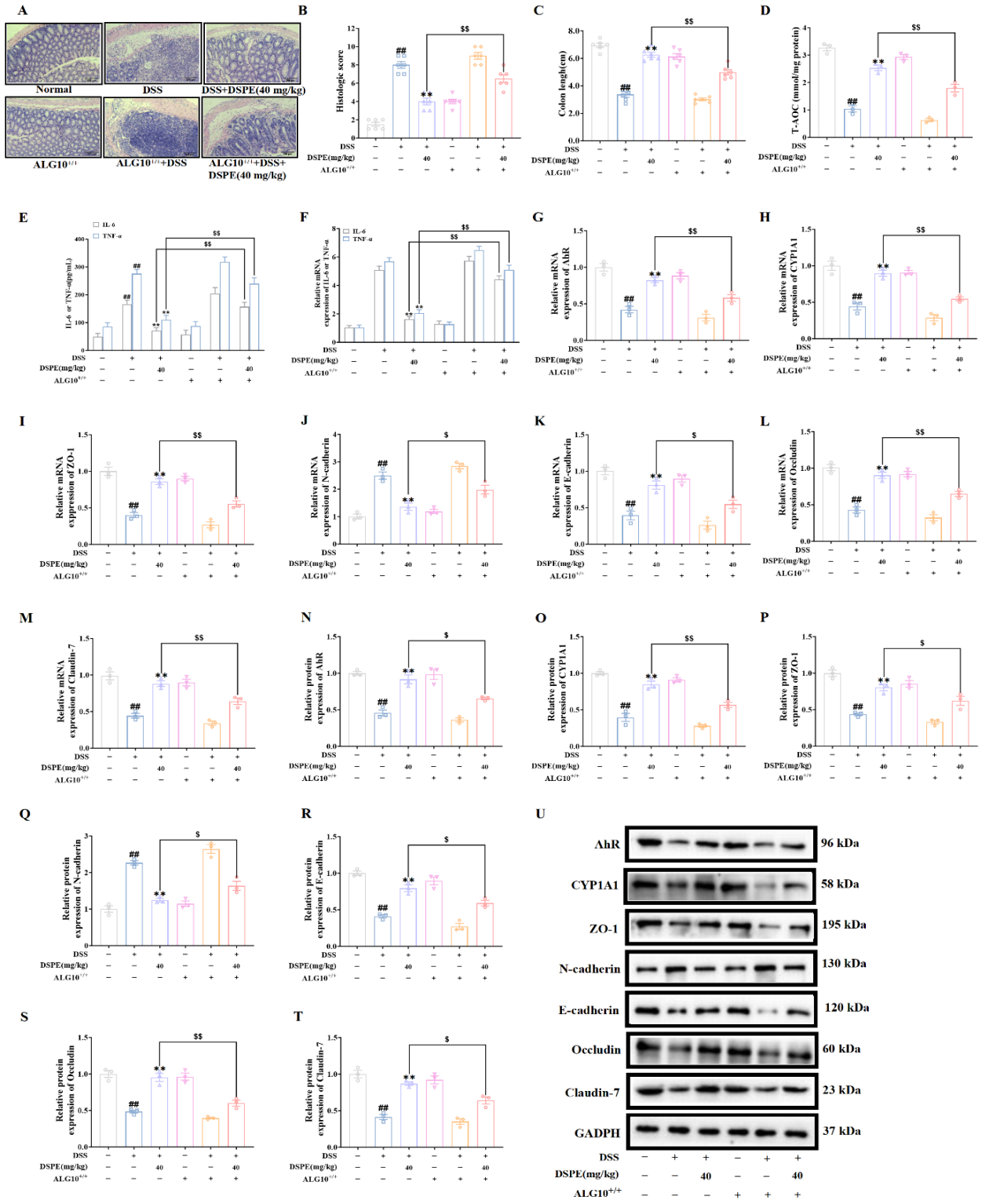


Fig. 11: The effect of ALG10 on the improvement of UC inflammation, oxidative stress, and intestinal epithelial dysfunction by regulating DSPE. (A) Representative colonic tissue H&E staining images (200×). (B) Histopathological score. (C) Colon length. (D) The level of T-AOC in colon tissue. (E) The protein expression levels of TNF-α and IL-6 in colon tissues. (F) The mRNA expression levels of TNF-α and IL-6 in colonic tissues. (G-M) The relative mRNA expression levels of AhR, CYP1A1, ZO-1, N-cadherin, E-cadherin, Occludin, and Claudin-7 in colon tissues. (N-T) Relative protein expression levels of AhR, CYP1A1, ZO-1, N-cadherin, E-cadherin, Occludin, and Claudin-7 in colon tissues. (U) Representative WB images of AhR, CYP1A1, ZO-1, N-cadherin, E-cadherin, Occludin, and Claudin-7 in colon tissues. Statistical data are presented as mean ± SEM; $^{\#\#}$P<0.01 compared with the Normal group; *P<0.05, **P<0.01 compared with the DSS group; $^{\$}$P<0.05, $^{\$\$}$P<0.01 compared with the DSS + DSPE (40mg/kg) group; ns indicates P>0.05.

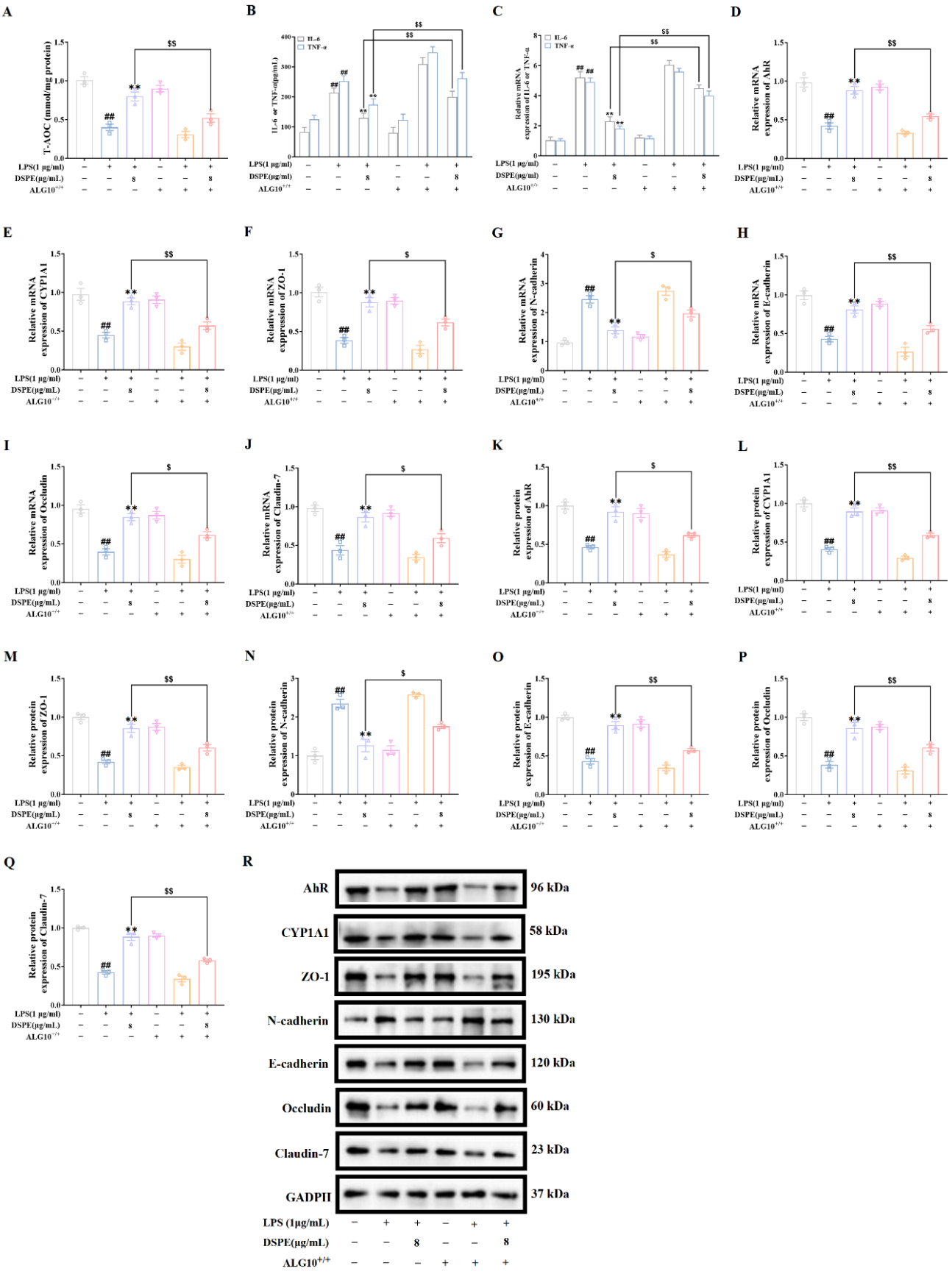


Fig. 12: The effect of ALG10 on the improvement of inflammation, oxidative stress, and intestinal epithelial dysfunction in Caco-2 cells by enhancing DSPE. (A) The T-AOC level of Caco-2 cells. (B) The protein expression levels of TNF-α and IL-6 in Caco-2 cells. (C) The mRNA expression levels of TNF-α and IL-6 in Caco-2 cells. (D-J) The relative mRNA expression levels of AhR, CYP1A1, ZO-1, N-cadherin, E-cadherin, Occludin, and Claudin-7 in Caco-2 cells. (K-Q) The relative protein expression levels of AhR, CYP1A1, ZO-1, N-cadherin, E-cadherin, Occludin, and Claudin-7 in Caco-2 cells. (R) Representative WB images of AhR, CYP1A1, ZO-1, N-cadherin, E-cadherin, Occludin, and Claudin-7 in Caco-2 cells. Statistical data are presented as mean ± SEM; $^{\#\#}$P<0.01 compared with the Normal group; *P<0.05, **P<0.01 compared with the DSS group; $^{\$}$P<0.05, $^{\$\$}$P<0.01 compared with the LPS + DSPE (8mg/kg) group; ns indicates P>0.05.

AhR has been shown to regulate multiple inflammatory pathways and is essential for maintaining intestinal mucosal homeostasis (Yu *et al*., 2018; Faber *et al*., 2022). AhR expression levels are lower in the colonic tissues of UC mice (Monteleone *et al*., 2011; Monteleone *et al*., 2016). In AhR knockout mice, the severity of DSS-induced colitis was significantly higher than that in wild-type (WT) mice, while intervention with the AhR agonist FICZ significantly alleviated DSS-induced UC symptoms (Wang *et al*., 2018). Further mechanistic studies showed that FICZ directly activates AhR in IECs, effectively reducing intestinal permeability, protecting epithelial structure, and thereby repairing DSS-induced barrier dysfunction (Yu *et al*., 2018).Similarly, Glehnia littoralis polysaccharides significantly ameliorated intestinal mucosal barrier damage in rats with ulcerative colitis by activating AhR to upregulate the expression of tight junction proteins and suppress inflammatory responses, and this protective effect could be abolished by an AhR antagonist (Geng *et al*., 2025). Astragalus polysaccharide effectively inhibited inflammatory responses and repaired the intestinal barrier by activating AhR to trigger autophagy in intestinal epithelial cells, thereby ameliorating experimental colitis (Ying *et al*., 2024). These studies indicate that activating AhR can effectively ameliorate intestinal mucosal barrier damage, thereby improving UC. In the present study, we observed that AhR antagonist treatment aggravated UC symptoms in mice and significantly inhibited DSPE-mediated activation of the AhR signaling pathway. More importantly, this antagonistic effect completely blocked the multiple protective effects of DSPE in the intestine, including the alleviation of oxidative stress damage. These results strongly indicate that DSPE ameliorates UC primarily through the activation of the AhR signaling pathway.

ALG10 is precisely defined as an asparagine-linked α-1,2-glucosyltransferase involved in N-glycosylation of eukaryotic proteins, playing a key role in tumor progression. Studies have shown that downregulation of glucosyltransferases can enhance the oxidative stress response of cells or tissues (Chong *et al*., 2002). Therefore, we hypothesized that ALG10 may be a key target of DSPE in ameliorating UC. To determine whether DSPE ameliorates intestinal epithelial dysfunction in UC by regulating ALG10, the present study established an ALG10 overexpression model in DSS- and LPS-induced UC models to verify this hypothesis. The results showed that ALG10 overexpression not only significantly reversed the therapeutic effects of DSPE in UC, including its inhibition of inflammation, attenuation of oxidative stress, and promotion of intestinal epithelial barrier repair, but also suppressed the upregulation of AhR and its downstream target CYP1A1. Notably, under specific AhR inhibition, the regulatory effect of DSPE on ALG10 was not affected. This phenomenon was consistently verified in both in vivo and in vitro experiments, indicating that DSPE-mediated suppression of ALG10 expression is independent of AhR. These results suggest that ALG10 is highly likely to act upstream of AhR. Based on these experimental results, we propose that DSPE may exerts its anti-UC effects by modulating the ALG10/AhR/CYP1A1 signaling pathway to effectively inhibit intestinal inflammatory responses and oxidative stress levels, and promote the restoration of intestinal epithelial barrier function.

The present study identified ALG10 as a potential target of DSPE and demonstrated that DSPE exerts anti-UC effects by modulating the ALG10/AhR/CYP1A1 signaling pathway, maintaining the integrity and function of the intestinal epithelial barrier. Nevertheless, this study also has certain limitations. Although DSPE showed significant therapeutic effects in UC models, the ALG10/AhR/CYP1A1 signaling pathway may be the sole pathway through which DSPE exerts its anti-UC effects. Since other signaling pathways have not yet been explored, a more comprehensive explanation of the anti-UC mechanism of DSPE cannot be provided. Since other signaling pathways have not yet been explored, the present study cannot yet provide a more comprehensive explanation of the mechanism underlying the anti-UC effects of DSPE. Moreover, this study merely suggests that ALG10 may act upstream of AhR, but cannot demonstrate a direct molecular interaction between the two, which warrants further in-depth investigation in the future. In addition, the sample size of n=6 per group in this study is relatively small, which may limit statistical power and reduce the confidence in the reported effects, and further verification in larger samples is needed in subsequent studies. In future studies, it is necessary to integrate molecular biology and systems biology approaches to elucidate the multi-target and multi-pathway mechanisms of DSPE in murine UC.

Conclusions: In conclusion, this study initially revealed the molecular mechanism through which DSPE protects intestinal epithelial barrier integrity and ameliorates UC by regulating the ALG10/AhR/CYP1A1 signalling pathway, providing crucial preliminary evidence for its development as a novel UC therapeutic agent and laying an important theoretical foundation for the high-value development and utilisation of durian shells.

Funding: This study received funding from the National Natural Science Foundation of China (82360646), the Natural Science Foundation of Guangxi (2024GXNSFAA010014, 2026GXNSFAA00640584), the President's Fund of Tarim University (TDZKBS202627, TDZKBS202630). Authors also appreciate the financial support from the Deanship of Scientific Research, Vice Presidency for Graduate Studies and Scientific Research, King Faisal University, Saudi Arabia (Grant No. KFU265703). The authors extend their appreciation to the Deanship of Research and Graduate Studies at King Khalid University for funding this work through Large Research Project under grant number (R. G. P. 2/185/46).

Authors contribution: XX, LC, XW: Writing–original draft, Methodology, Formal analysis, Investigation, Validation, Conceptualization; MY, RW, SZ, YZ, MAR, EHI: Investigation, Visualization, Methodology, Data curation, Conceptualization; SD**:** Formal analysis, Data curation, Supervision, Conceptualization; YW: Project administration, Writing–review & editing, Investigation, Funding acquisition, Conceptualization.

REFERENCES

Aviello G, Singh AK, O'Neill S, *et al*., 2019. Colitis susceptibility in mice with reactive oxygen species deficiency is mediated by mucus barrier and immune defense defects. Mucosal Immunology 12(6):1316-1326.

Cheng Z, Zhou Y, Xiong X, *et al*., 2024. Traditional herbal pair Portulacae Herba and Granati Pericarpium alleviates DSS-induced colitis in mice through IL-6/STAT3/SOCS3 pathway. Phytomedicine 126:155283.

Chong J, Baltz R, Schmitt C, *et al*., 2002. Downregulation of a pathogen-responsive tobacco UDP-Glc:phenylpropanoid glucosyltransferase reduces scopoletin glucoside accumulation, enhances oxidative stress, and weakens virus resistance. The Plant Cell 14(5):1093-1107.

De Angelis PM, Dorg L, Pham S, *et al*., 2021. DNA repair protein expression and oxidative/nitrosative stress in ulcerative colitis and sporadic colorectal cancer. Anticancer Research 41(7):3261-3270.

Dong G, Pang X, Wang X, *et al*., 2024. Protective effect of Huanglian Pingwei San on DSS-induced ulcerative colitis in mice through amelioration of the inflammatory response and oxidative stress. Frontiers in Pharmacology 15:1484532.

Dong L, Du H, Zhang M, *et al*., 2022. Anti-inflammatory effect of Rhein on ulcerative colitis via inhibiting PI3K/Akt/mTOR signaling pathway and regulating gut microbiota. Phytotherapy Research 36(5):2081-2094.

Faber SC, Lahoti TS, Taylor ER, *et al*., 2022. Current therapeutic landscape and safety roadmap for targeting the aryl hydrocarbon receptor in inflammatory gastrointestinal indications. Cells 11(10):1708.

Geng X, Liu J, Feng H, et al., 2025. Glehnia littoralis polysaccharides alleviate lung and intestinal mucosal barrier damage in rats with ulcerative colitis via aryl hydrocarbon receptor activation. International Journal of Biological Macromolecules 327(Pt 2):147318.

Grishanova AY, Perepechaeva ML, 2022. Aryl hydrocarbon receptor in oxidative stress as a double agent and its biological and therapeutic significance. International Journal of Molecular Sciences 23(12):6719.

Jeon YD, Lee JH, Lee YM, *et al*., 2020. Puerarin inhibits inflammation and oxidative stress in dextran sulfate sodium-induced colitis mice model. Biomedicine & Pharmacotherapy 124:109847.

Kobayashi T, Siegmund B, Le Berre C, *et al*., 2020. Ulcerative colitis. Nature Reviews Disease Primers 6(1):74-92.

Lamas B, Richard ML, Leducq V, *et al*., 2016. CARD9 impacts colitis by altering gut microbiota metabolism of tryptophan into aryl hydrocarbon receptor ligands. Nature Medicine 22(6):598-605.

Li C, Yang F, Wu Z, *et al*., 2025. Coptisine alleviates intestinal barrier dysfunction and inflammation in TNBS-induced colitis rats and LPS-stimulated human intestinal Caco-2 cells. International Immunopharmacology 167:115697.

Li MX, Li MY, Lei JX, *et al*., 2022a. Huangqin decoction ameliorates DSS-induced ulcerative colitis: Role of gut microbiota and amino acid metabolism, mTOR pathway and intestinal epithelial barrier. Phytomedicine 100:154052.

Li XQ, Ouyang W, Jiang YQ, *et al*., 2023a. Dextran-sulfate-sodium-induced colitis-ameliorating effect of aqueous *Phyllanthus emblica* L. extract through regulating colonic cell gene expression and gut microbiomes. Journal of Agricultural and Food Chemistry 71(18):6999-7008.

Li YY, Wang XJ, Su YL, *et al*., 2022b. Baicalein ameliorates ulcerative colitis by improving intestinal epithelial barrier via AhR/IL-22 pathway in ILC3s. Acta Pharmacologica Sinica 43(6):1495-1507.

Li ZY, Lin LH, Liang HJ, *et al*., 2023b. *Lycium barbarum* polysaccharide alleviates DSS-induced chronic ulcerative colitis by restoring intestinal barrier function and modulating gut microbiota. Annals of Medicine 55(2):2290213.

Liu S, Song J, Yang W, *et al*., 2025. Research progress on structural characteristics, biological activities and degradation of *Lycium barbarum* polysaccharides. Chinese Traditional and Herbal Drugs 56(4):1440-1455.

Luo L, Zhou Z, Xue J, *et al*., 2018. *Bletilla striata* polysaccharide has a protective effect on intestinal epithelial barrier disruption in TAA-induced cirrhotic rats. Experimental and Therapeutic Medicine 16(3):1715-1722.

Martini E, Krug SM, Siegmund B, *et al*., 2017. Mend your fences: The epithelial barrier and its relationship with mucosal immunity in inflammatory bowel disease. Cellular and Molecular Gastroenterology and Hepatology 4(1):33-46.

Monteleone I, Rizzo A, Sarra M, *et al*., 2011. Aryl hydrocarbon receptor-induced signals up-regulate IL-22 production and inhibit inflammation in the gastrointestinal tract. Gastroenterology 141(1):237-248.e1.

Monteleone I, Zorzi F, Marafini I, *et al*., 2016. Aryl hydrocarbon receptor-driven signals inhibit collagen synthesis in the gut. European Journal of Immunology 46(4):1047-1057.

Neurath MF, 2019. Targeting immune cell circuits and trafficking in inflammatory bowel disease. Nature Immunology 20(8):970-979.

Schulzke JD, Ploeger S, Amasheh M, *et al*., 2009. Epithelial tight junctions in intestinal inflammation. Annals of the New York Academy of Sciences 1165:294-300.

Sun X, Guo R, Kou Y, *et al*., 2023. Inhibition of ice recrystallization by tamarind (*Tamarindus indica* L.) seed polysaccharide and molecular weight effects. Carbohydrate Polymers 301(Pt B):120358.

Sun Y, Shi X, Zheng X, *et al*., 2019. Inhibition of dextran sodium sulfate-induced colitis in mice by baker's yeast polysaccharides. Carbohydrate Polymers 207:371-381.

Uwada J, Nakazawa H, Muramatsu I, *et al*., 2023. Role of muscarinic acetylcholine receptors in intestinal epithelial homeostasis: Insights for the treatment of inflammatory bowel disease. International Journal of Molecular Sciences 24(7):6508.

Waly NE, Stokes CR, Gruffydd-Jones TJ, *et al*., 2004. Immune cell populations in the duodenal mucosa of cats with inflammatory bowel disease. Journal of Veterinary Internal Medicine 18(6):816.

Wang Q, Yang K, Han B, *et al*., 2018. Aryl hydrocarbon receptor inhibits inflammation in DSS-induced colitis via the MK2/p-MK2/TTP pathway. International Journal of Molecular Medicine 41(2):868-876.

Wang X, Xie X, Li Y, *et al*., 2024. Quercetin ameliorates ulcerative colitis by activating aryl hydrocarbon receptor to improve intestinal barrier integrity. Phytotherapy Research 38(1):253-264.

Wang Y, Zhang J, Zhang B, *et al*., 2023. Modified Gegen Qinlian decoction ameliorated ulcerative colitis by attenuating inflammation and oxidative stress and enhancing intestinal barrier function in vivo and in vitro. Journal of Ethnopharmacology 313:116538.

Wei Q, Jiang H, Zeng J, *et al*., 2025. Quercetin protected the gut barrier in ulcerative colitis by activating aryl hydrocarbon receptor. Phytomedicine 140:156633.

Wu H, Li YL, Wang Y, *et al*., 2025. Anemoside B4 alleviates ulcerative colitis by attenuating intestinal oxidative stress and NLRP3 inflammasome via activating aryl hydrocarbon receptor through remodeling the gut microbiome and metabolites. Redox Biology 85:103746.

Xu D, Ma R, Ju Y, *et al*., 2022a. Cholesterol sulfate alleviates ulcerative colitis by promoting cholesterol biosynthesis in colonic epithelial cells. Nature Communications 13(1):4428.

Xu XT, Wang HD, Li XH, *et al*., 2022b. A novel ALG10/TGF-β positive regulatory loop contributes to the stemness of colorectal cancer. Aging 14(11):4858-4873.

Xu Y, Zhang X, Yan XH, *et al*., 2019. Characterization, hypolipidemic and antioxidant activities of degraded polysaccharides from Ganoderma lucidum. International Journal of Biological Macromolecules 135:706-716.

Yang C, Du Y, Li Q, *et al*., 2024. Fructo-oligosaccharides alleviated ulcerative colitis via gut microbiota-dependent tryptophan metabolism in association with aromatic hydrocarbon receptor activation in mice. Journal of Agricultural and Food Chemistry 72(50):27912-27922.

Ying Y, Song LY, Pang WL, et al., 2024. Astragalus polysaccharide protects experimental colitis through an aryl hydrocarbon receptor-dependent autophagy mechanism. British Journal of Pharmacology 181(5):681-697.

Yu M, Wang Q, Ma Y, *et al*., 2018. Aryl hydrocarbon receptor activation modulates intestinal epithelial barrier function by maintaining tight junction integrity. International Journal of Biological Sciences 14(1):69-77.

Yue L, Wang W, Wang Y, *et al*., 2016. Bletilla striata polysaccharide inhibits angiotensin II-induced ROS and inflammation via NOX4 and TLR2 pathways. International Journal of Biological Macromolecules 89:376-388.

Zhang C, Gao F, Gan S, *et al*., 2019. Chemical characterization and gastroprotective effect of an isolated polysaccharide fraction from Bletilla striata against ethanol-induced acute gastric ulcer. Food and Chemical Toxicology 131:110539.

Zhang D, Wu J, Feng H, *et al*., 2025. Gastrodin ameliorates ulcerative colitis via modulating gut microbial tryptophan metabolism and AhR/NLRP3 pathway. Phytomedicine 147:157217.

Zhou R, Huang K, Chen S, *et al*., 2024. Zhilining Formula alleviates DSS-induced colitis through suppressing inflammation and gut barrier dysfunction via the AHR/NF-κBp65 axis. Phytomedicine 129:155571.